LIMNOLOGY AND OCEANOGRAPHY
Letters

ASLO
Open Access

Limnology and Oceanography Letters 2024

doi: 10.1002/lol2.10399

LETTER

Bivalve tissues as a recorder of multidecadal global anthropogenic and climate-mediated change in coastal areas

Camilla Liénart[1]* *Alan Fournioux*[1] *Andrius Garbaras*[2] *Arnaud Lheureux*[3] *Hugues Blanchet*[1] *Nicolas Briant*[4] *Stanislas F. Dubois*[5] *Aline Gangnery*[5] *Anne Grouhel Pellouin*[4] *Pauline Le Monier*[4] *Xavier De Montaudouin*[1] *Nicolas Savoye*[1]

[1]Université de Bordeaux, CNRS, Bordeaux INP, EPOC, UMR 5805, Pessac, France; [2]Center for Physical Sciences and Technology, Vilnius, Lithuania; [3]Laboratoire de Biologie des Organismes et Écosystèmes Aquatiques (BOREA), MNHN, CNRS, IRD, SU, UCN, UA, CP53, Paris, France; [4]Ifremer, CCEM Contamination Chimique des Écosystèmes Marins, Nantes, France; [5]Ifremer, DYNECO, Plouzané, France

Scientific Significance Statement

Global change affects physicochemical and biological compartments of coastal ecosystems from global to local scales. However, the multiple and interacting effects make it challenging to identify what causes ecosystem responses. By using bivalve species as a recorder of environmental changes, this study provides the evidence for global effects of anthropogenic activities (bivalves reflect the isotopic signal of atmospheric CO_2, which is directly affected by anthropogenic activities) and of climate change on coastal ecosystems at global scale, with possible cumulative, synergistic or antagonistic regional and/or local effects. This research is contributing to crucial understanding of coastal ecosystems responses to environmental and climate change.

Abstract

Recent rapid changes in climate and environmental conditions have significantly impacted coastal ecosystem functioning. However, the complex interplay between global and local effects makes it challenging to pinpoint the primary drivers. In a multi-ecosystem study, we analyzed pluri-decadal trends of bivalve-$\delta^{13}C$ as recorder of global environmental changes. These trends were correlated with large-scale natural and anthropogenic climate proxies to identify whether coastal biota responded to global effects. Our findings revealed decreasing bivalve-$\delta^{13}C$ trends in all sea regions, mainly linked with increased temperature and atmospheric-CO_2

*Correspondence: camilla.lienart@u-bordeaux.fr

Associate editor: Dick van Oevelen

Author Contribution Statement: LC performed conceptualization, methodology, investigation, formal analysis, visualization, writing–original draft preparation (lead). FA involved in investigation, formal analysis, visualization, review, and editing. G. Andrius did investigation. LA did investigation, formal analysis, review, and editing. BH performed conceptualization, methodology, review, and editing. BN performed investigation, review, and editing. FDS performed conceptualization, methodology, review, and editing. G. Aline performed investigation, review, and editing. GPA performed methodology, investigation, review, and editing. LMP did Investigation. deMX performed conceptualization, methodology, review, and editing. SN performed conceptualization, methodology, writing–review and editing.

Data Availability Statement: Data and metadata are uploaded in a freely accessible repository (Figshare) under the permanent identifier https://doi.org/10.6084/m9.figshare.24884871.v1.

Additional Supporting Information may be found in the online version of this article.

concentrations, the later generating a decrease in atmospheric-CO_2 $\delta^{13}C$ values (Suess effect) because of fossil-fuel burning. After removing the Suess effect from bivalve-$\delta^{13}C$ trends, ongoing global climate variability continues to affect most ecosystems, possibly intensified by combined, interacting regional or local effects. These results highlight the need to consider large-scale effects to fully understand ecosystem and food web responses to the multiple effects of global change.

Over the past decades, the world ocean has undergone rapid climate and environmental changes with significant consequences on ecosystem functioning and services (Halpern et al. 2008; Bauer et al. 2013; Bartley et al. 2019; Benedetti et al. 2021; Cael et al. 2023). Coastal marine ecosystems form a dynamic land-ocean interface holding substantial ecological and economic value (Barbier et al. 2011). As the ultimate receptacle of dissolved and particulate continental inputs from natural and anthropogenic origin, these ecosystems are highly productive yet particularly sensitive to the multiple and interacting pressures of global change acting at various spatial and temporal scales (Harley et al. 2006). Climate and human-induced changes in precipitations, river discharge, nutrients load or land use, alter organic matter transformation and ultimately nutrient cycling and productivity along the land-ocean continuum (Milliman et al. 2008; Bauer et al. 2013). A key challenge remains to understand how the different components of global change affect coastal ecosystems responses.

Global change refers to planetary-scale changes in the Earth system encompassing interacting physicochemical and biological compartments, and human societies. It comprises the global climate (i.e., natural and anthropogenic components) and other, mostly local, human activities (e.g., land use, pollution) that affect ecosystems. Local changes may interact with global climate-induced changes in antagonistic, cumulative, or synergistic ways, thereby exacerbating ecosystems response (Harley et al. 2006; Cabral et al. 2019). Therefore, disentangling global from regional and or local effects is crucial for the understanding of coastal ecosystem functioning, especially to improve predictive scenarios and adapt management and conservation strategies.

Carbon is the primary currency in addressing global change. Carbon stable isotope ($\delta^{13}C$) is commonly used to understand physical–chemical processes in the ocean: it helps tracing organic matter origin and fate (Bristow et al. 2013) and to reveal global anthropogenic impact such as direct effect of increasing carbon dioxide (CO_2) emissions from anthropogenic activities (Quay et al. 2007). The CO_2 emitted by fossil fuels burning (e.g., coal, oil, and natural gas) has a lower proportion of ^{13}C than the CO_2 naturally present in the atmosphere and dilute the overall concentration of ^{13}C at global scale, creating the Suess effect (i.e., decline in global atmospheric $\delta^{13}C$ values by 1.8‰ since the industrial revolution in 1850 to present day; Keeling 1979; Gruber et al. 1999; Graven et al. 2017; Dombrosky 2020). Low $\delta^{13}C$-CO_2 dissolved in seawater is biologically incorporated by primary producers during photosynthesis and propagates along the food web (e.g., Schloesser et al. 2009; Liénart et al. 2022), and potentially masks local influence of ^{13}C-depleted sources (e.g., continental material from rivers; Liénart et al. 2017, 2022). Increasing anthropogenic CO_2 emissions also indirectly affects marine ecosystems through temperature increase leading, for example, to altered CO_2 solubility in water, phytoplankton phenology or precipitation patterns and river runoffs (Pörtner et al. 2005; Gittings et al. 2018; van Vliet et al. 2013).

Bivalve species, as bioindicators for environmental monitoring, offer an integrated view of the environmental conditions of their habitat through sessile, filter-feeding lifestyles (Briant et al. 2021; Karlson and Faxneld 2021; Chahouri et al. 2023). Measuring $\delta^{13}C$ of bivalve tissues allows to trace dietary carbon resources (Magni et al. 2013) and its flows in food webs over space and time (Vander Zanden and Rasmussen 1999; Corman et al. 2018), and to understand ecological consequences of environmental changes in ecosystem functioning (Liénart et al. 2020). Bivalve-$\delta^{13}C$ is primarily influenced by local dietary changes and physiological processes but global effects, like the Suess effect, can mask these processes in long-term isotope trends, hindering for precise interpretations of change (Clark et al. 2021). Considering Suess effect in isotope data is critical to unravel pure anthropogenic effects (fossil fuel burning) from other global and regional/local pressures.

Previous studies addressing global change from pluri-decadal trends of bivalve-$\delta^{13}C$ found a link to climate change (Briant et al. 2018; Corman et al. 2018), with only few statistical evidence for indirect climate effects (Liénart et al. 2020, 2022). However, no study had distinctly estimated and removed global effects, particularly the Suess effect, before further examining other processes. Our study address whether pluri-decadal trends in bivalve-$\delta^{13}C$ are due to the Suess effect, and if, when corrected, other global effects persist. In a multiecosystem approach, we measured $\delta^{13}C$ in mussels and oysters across 32 stations in six contrasted sea regions, over four-decades time series (1981–2021). We correlated multidecadal changes in bivalve-$\delta^{13}C$ with time-series of large-scale anthropogenic and climate proxies to identify global effects. By studying bivalve-$\delta^{13}C$ time-series as a record of environmental changes, this study examines global effects of anthropogenic activities (i.e., reflect the isotopic signal of increased atmospheric CO_2) and of climate change on coastal temperate ecosystems at broad spatial scale.

Methods

Archived samples

Since the late 1970s, the French National Monitoring Network "ROCCH" ("Réseau d'Observation de la Contamination CHimique," operated by IFREMER) uses bivalves from three different species as bioindicators of chemical contamination: the Pacific oyster *Crassostrea gigas*, and the blue mussels *Mytilus edulis* and *Mytilus galloprovincialis* (Fig. 1; see Supporting Information S1 for detailed sampling protocol). For the purpose of this study, we analyzed 1136 archived bivalves soft-tissues samples (total soft-tissues) from the ROCCH network, across 32 stations of six sea regions (Fig. 1, English Channel; Western Brittany; Northern Bay of Biscay; Central Bay of Biscay; Arcachon Lagoon; Gulf of Lion) spanning 21–40 years over the period 1981–2021 (one sample per year, collected in mid-February ± 3 weeks, i.e., during low growth, mostly during non-reproductive period, to minimize the effects of lipids associated with gametogenesis as lipids are ^{13}C depleted, Post et al. 2007). The stations were specifically selected to reflect environmental gradients on both large and local scale (Lheureux et al. 2023), for example, tidal regimes (microtidal to megatidal), climates (temperate, oceanic, mediterranean), trophic status (oligotrophic to eutrophic), continental influence (gradients of influence of rivers).

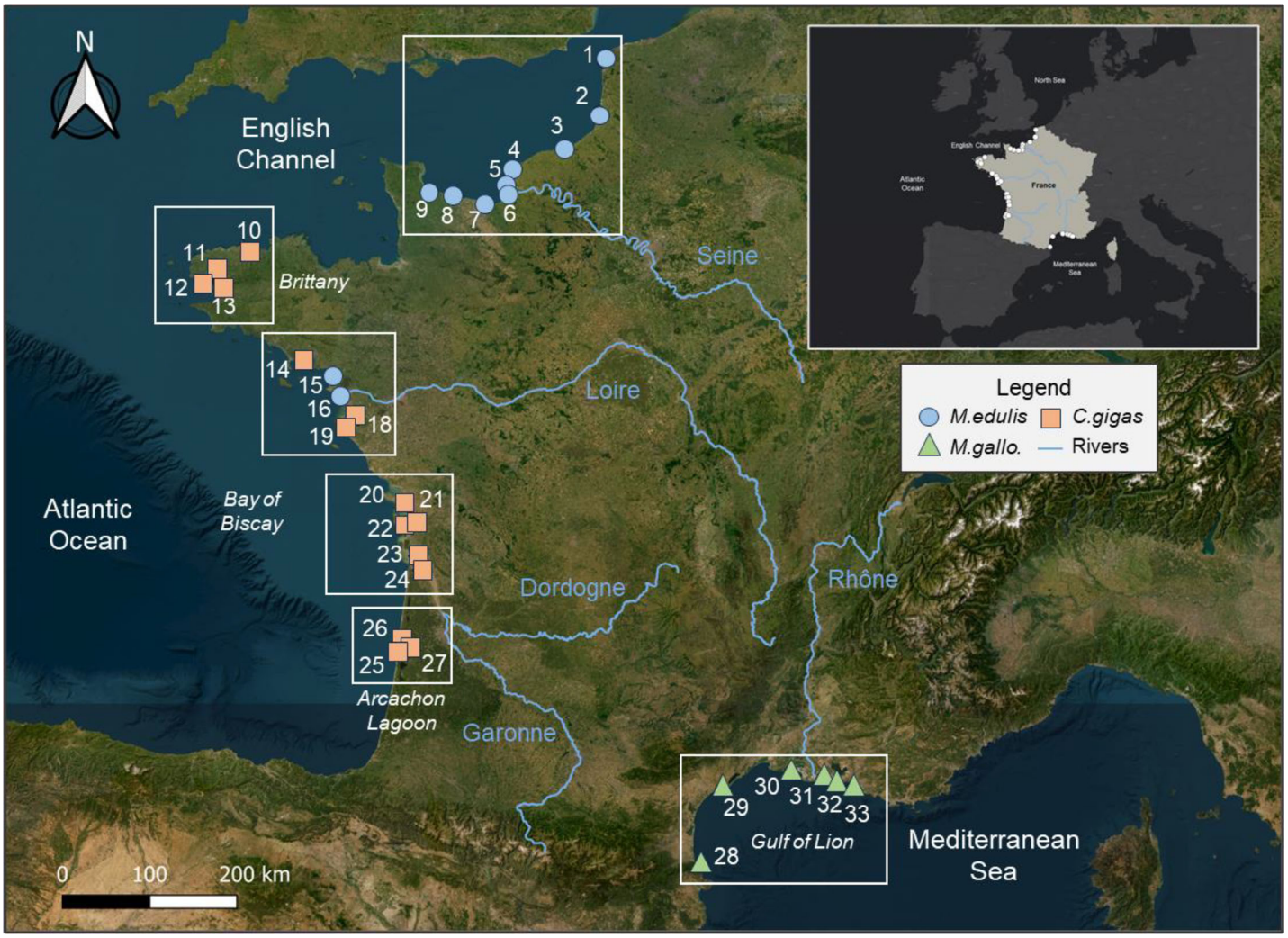

Fig. 1. Geographical location of the 32 stations sampled for bivalves (*M. edulis*: blue circles, *M. galloprovincialis*: green triangles, *C. gigas*: orange squares) in the six sea regions (English Channel; Western Brittany; Northern Bay of Biscay; Central Bay of Biscay; Arcachon Lagoon; Gulf of Lion) over the period 1981–2021. At each station, only one of the three species was sampled: *M. edulis* in the English Channel and at two stations of the Northern Bay of Biscay, *C. gigas* in Western Brittany, Central Bay of Biscay, Arcachon Lagoon and three stations of the Northern Bay of Biscay, and *M. galloprovincialis* in the Gulf of Lion. The main river influencing the regions are represented by blue lines. The full list of station names is available in Supporting Information S1. Note that there is no Station number 17.

Carbon stable isotope analysis

We analyzed aliquots of 400–700 μg of bivalve tissues of each archived sample for $\delta^{13}C$ at the Center for Physical Science and Technology (Vilnius, Lithuania) with a Flash EA 1112 Series Elemental Analyzer (Thermo Finnigan) connected to a DeltaV Advantage Isotope Ratio Mass Spectrometer (Thermo Fisher). Results are expressed in per mil (‰) deviation from international references (see Supporting Information S1). Analytical precision was <0.15‰. Isotope data are available in the Figshare repository under the DOI 10.6084/m9.figshare.24884871.

Proxies for global environmental change

We compiled publicly available data over the period 1981–2021 for five hydro-climatic teleconnection indices representing climate patterns in the Northern hemisphere (see Supporting Information Fig. S1). Two indices are based on temperatures: the Atlantic Multidecadal Oscillation (AMO; Enfield et al. 2001) represents changes in the north Atlantic Ocean surface temperature after removing the anthropogenic component (effect of increasing greenhouse gases), whereas the Northern Hemisphere temperature (NHT) anomalies are calculated from North Atlantic 1901–2000 temperature average. Three indices are based on atmospheric pressures: the North Atlantic Oscillation (NAO; Hurrell 1995; Hurrell and Deser 2009) corresponds to the pressure difference between the Azores High and Icelandic Low; the East Atlantic Pattern (EAP; Barnston and Livezey 1987) values consist in a north–south dipole of pressure anomalies centered on the north Atlantic from east to west; the Arctic Oscillation (AO) is based on atmospheric pressures and is related to the Arctic climate and its southern incursions (Higgins et al. 2000). We used globally averaged North-Hemisphere atmospheric CO_2 concentrations (CO_{2atm}; Lan et al. 2023) and $\delta^{13}C$ of atmospheric CO_2 ($\delta^{13}C$-CO_{2atm}; Graven et al. 2017) as global effect proxies resulting from anthropogenic activities. For each proxy and time series, we recalculated yearly averages based on the 12 months preceding bivalve sampling in order to integrate a temporal lag in bivalve-$\delta^{13}C$ (except for $\delta^{13}C$-CO_{2atm} and seawater $\delta^{13}C$-CO_2, see below, where the previous calendar year was selected). Data origin and calculation details are available in Supporting Information S1.

The Suess effect

A step-by-step calculation of Suess effect is available in Supporting Information S1. Briefly, we calculated $\delta^{13}C$ of CO_2 dissolved in seawater ($\delta^{13}C$-CO_{2aq}) for each region by adding the corresponding regional isotopic fractionation (ε) value to global $\delta^{13}C$-CO_{2atm} for each year on the period 1980–2021 (Table S1). The fractionation between gaseous and dissolved CO_2 phases was calculated from the equation of Vogel et al. (1970) as given by Mook (2000), and Zeebe and Wolf-Gladrow (2001): $\varepsilon_{d/g} = -373/T + 0.19‰$ (T: absolute temperature in Kelvin). Despite differences in temperature within each time series and between regions, differences in calculated ε, hence in $\delta^{13}C$-CO_{2aq} values was much lower than the analytical precision for bivalves-$\delta^{13}C$ (see Supporting Information S1). Therefore, we used the average $\delta^{13}C$-CO_{2aq} value of all regions as a proxy to compare with bivalves-$\delta^{13}C$ in statistical tests. Finally, we calculated regional slopes of $\delta^{13}C$-CO_{2aq} (i.e., the Suess effect) which was the same for all regions (−0.243‰ decade^{-1}, Table S1), and removed it from bivalve-$\delta^{13}C$ cumulatively for each year (starting from year 1981) to obtain Suess-corrected bivalve-$\delta^{13}C$ (bivalve-$\delta^{13}C_{corr}$) for each station.

Equilibrium between $\delta^{13}C$-CO_{2atm} and $\delta^{13}C$-CO_{2aq}, and $\delta^{13}C$ in phytoplankton and bivalves (i.e., tissue turnover) are possible processes altering $\delta^{13}C$ signal propagation to bivalves. Considering that these lags are constant over years, it does not affect the multidecadal $\delta^{13}C$ trends we are investigating. Also, we did not consider seasonal variation in atmospheric CO_2, nor in the $\delta^{13}C$ of aquatic CO_2 linked to phytoplankton activity as we were looking at long-term trends in annual means. Hence, we considered equilibrium between atmosphere and seawater and calculated the trends of $\delta^{13}C$-CO_{2aq} as if the Suess effect was the only process occurring (i.e., considering physical–chemical processes only, Affek and Yakir 2014).

Statistical analyses

We examined unidirectional temporal trends in bivalve-$\delta^{13}C$ times series for each station with Mann-Kendall tests corrected for autocorrelation (R-package "modifiedmk," Patakamuri and O'Brien 2021). We applied linear models to calculate the value of the slope (in ‰ decade^{-1}). Over the same time period, we evaluated relationships (1) in bivalve-$\delta^{13}C$ time series between pairs of stations and (2) between bivalve-$\delta^{13}C$ time series and global proxies using Spearman two-sided correlation tests (p-values corrected for multiple testing with Benjamini–Hochberg procedure). For reliable comparison between datasets, we tested the trends on a common period of three decades (1990–2021) corresponding to 30 ± 2 years (criterion met for 28 stations), whereas correlations were performed on complete datasets. Statistical analyses were performed with the R software (R Core Team 2022).

Results

Pluri-decadal trends in bivalve-$\delta^{13}C$

During a shared period of 30 ± 2 years (1990–2021), bivalve-$\delta^{13}C$ signal exhibited a significant decrease at 93% of the stations (26/28; Fig. 2, Table 1). The average decrease was −0.58 ± 0.24‰ decade^{-1}, ranging from −1.08 to −0.22‰ decade^{-1} (i.e. −3.24 to −0.65‰ over 30 years). The decrease was not significant at only three stations (two in English Channel, one in Northern Bay of Biscay, over 30 years). Within each region, between station pairs, there were 80–100% of significant correlations in bivalve-$\delta^{13}C$ in

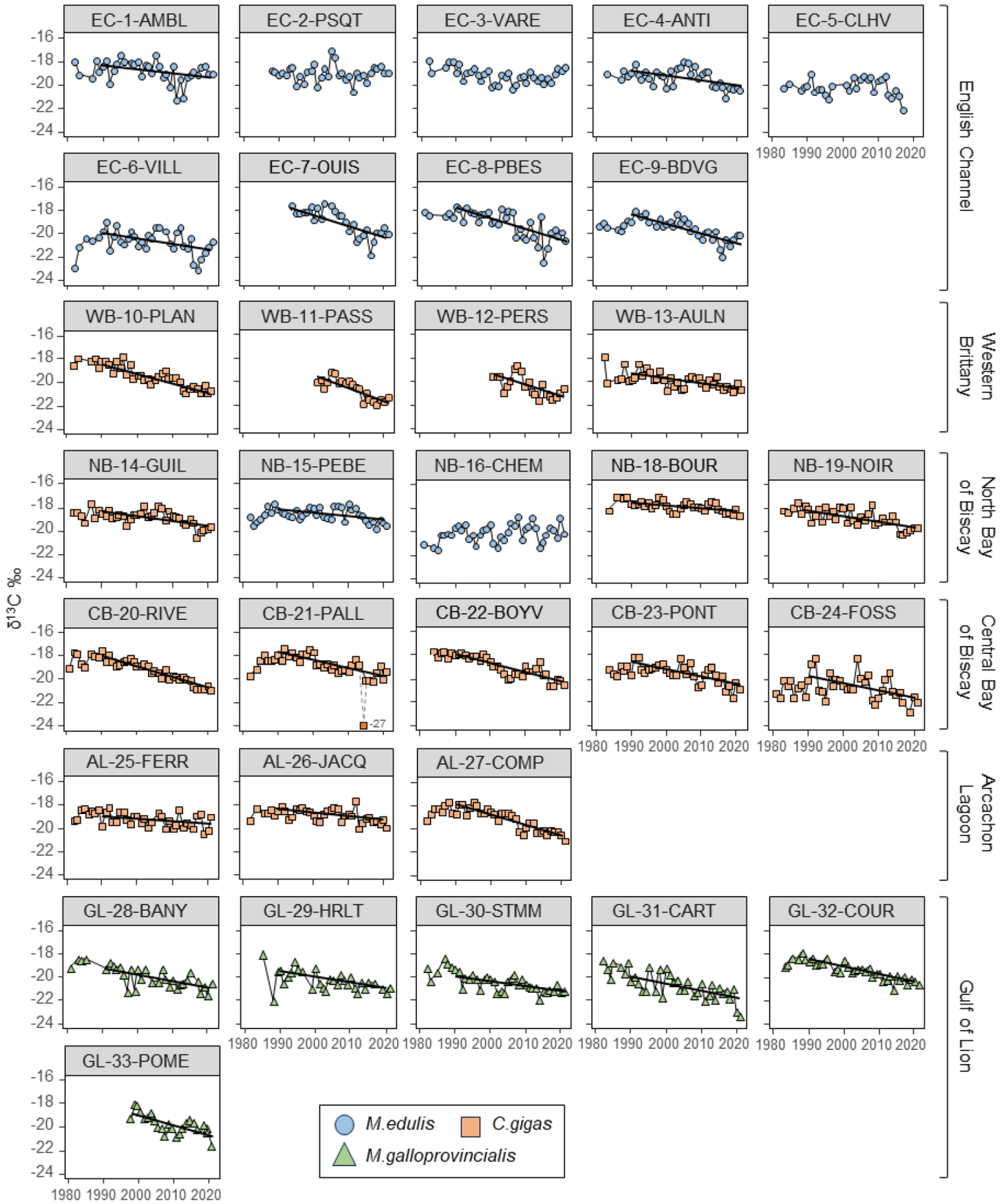

Fig. 2. Pluri-decadal variability in bivalve-$\delta^{13}C$ over the period 1981–2021 for the 32 stations of the six sea regions. Black lines correspond to significant trends (calculated on the period 1990–2021; Mann-Kendall tests; p-value < 0.05). One outlier (CB-21-PALL in 2014, −27‰) was removed for statistical tests. Colors corresponds to species.

Table 1. Raw values (mean ± SD, over the total dataset; *n* total = number of years of the time series) and decadal slopes of bivalve $\delta^{13}C$ (dark gray) and bivalve $\delta^{13}C$ corrected for the Suess effect (light gray, $\delta^{13}C_{corr}$) calculated over a common period of 30 ± 2 years (1990–2021).

		$\delta^{13}C$ raw values			Years		Slope (‰ decade^{-1})	
		n total	Average ± sd	n	Start	End	$\delta^{13}C$	$\delta^{13}C_{corr}$
English Channel (EC)	EC-1-AMBL	36	−18.8 ± 0.9	31	1990	2021	**−0.37**	−0.13
	EC-2-PSQT	34	−18.9 ± 0.7	32	1990	2021	0.04	**0.28**
	EC-3-VARE	37	−19.1 ± 0.6	32	1990	2021	−0.04	0.20
	EC-4-ANTI	36	−19.3 ± 0.8	32	1990	2021	**−0.44**	−0.19
	EC-5-CLHV	*29*	*−20.1 ± 0.7*	*25*	*1990*	*2017*	*−0.15*	*0.09*
	EC-6-VILL	36	−20.7 ± 1.0	31	1990	2021	**−0.51**	−0.27
	EC-7-OUIS	27	−19.0 ± 1.1	27	1994	2021	**−1.08**	**−0.84**
	EC-8-PBES	37	−19.1 ± 1.2	32	1990	2021	**−0.93**	**−0.69**
	EC-9-BDVG	37	−19.5 ± 0.9	30	1990	2021	**−0.84**	**−0.59**
Western Brittany (WB)	WB-10-PLAN	37	−19.5 ± 1.0	32	1990	2021	**−0.83**	**−0.59**
	WB-11-PASS	*21*	*−20.6 ± 0.8*	*21*	*2001*	*2021*	***−1.13***	***−0.89***
	WB-12-PERS	*21*	*−20.3 ± 0.9*	*21*	*2001*	*2021*	***−0.93***	***−0.69***
	WB-13-AULN	38	−19.8 ± 0.7	32	1990	2021	**−0.40**	−0.16
Northern Bay of Biscay (NB)	NB-14-GUIL	39	−18.8 ± 0.6	32	1990	2021	**−0.39**	−0.15
	NB-15-PEBE	40	−18.6 ± 0.6	32	1990	2021	**−0.27**	−0.03
	NB-16-CHEM	39	−20.1 ± 0.7	32	1990	2021	0.04	0.28
	NB-18-BOUR	37	−17.9 ± 0.8	32	1990	2021	**−0.23**	0.01
	NB-19-NOIR	38	−18.8 ± 0.7	32	1990	2021	**−0.49**	−0.24
Central Bay of Biscay (CB)	CB-20-RIVE	40	−19.1 ± 1.0	32	1990	2021	**−0.94**	**−0.69**
	CB-21-PALL	38	−18.7 ± 0.7	31	1990	2021	**−0.67**	**−0.42**
	CB-22-BOYV	38	−18.9 ± 0.9	32	1990	2021	**−0.79**	**−0.54**
	CB-23-PONT	38	−19.5 ± 0.8	32	1990	2021	**−0.63**	**−0.38**
	CB-24-FOSS	40	−20.7 ± 1.0	31	1990	2021	**−0.63**	**−0.38**
Arcachon lagoon (AL)	AL-25-FERR	39	−19.2 ± 0.6	31	1990	2021	**−0.22**	0.02
	AL-26-JACQ	38	−18.8 ± 0.5	32	1990	2021	**−0.32**	−0.08
	AL-27-COMP	40	−19.1 ± 0.9	32	1990	2021	**−0.91**	**−0.67**
Gulf of lion (GL)	GL-28-BANY	32	−19.9 ± 0.9	28	1991	2021	**−0.55**	**−0.30**
	GL-29-HRLT	31	−20.2 ± 0.8	28	1990	2021	**−0.48**	−0.24
	GL-30-STMM	38	−20.3 ± 0.8	32	1990	2021	**−0.44**	**−0.19**
	GL-31-CART	37	−20.6 ± 1.1	30	1990	2021	**−0.63**	**−0.39**
	GL-32-COUR	37	−19.3 ± 0.8	31	1990	2021	**−0.64**	**−0.40**
	GL-33-POME	*24*	*−19.8 ± 0.8*	*24*	*1998*	*2021*	***−0.85***	***−0.61***

Slope values were calculated from linear models and values are expressed in permille per decade. Significant slopes are in bold (Mann-Kendall tests; *p*-value <0.05). Time series that do not match time length requirements of 30 ± 2 years are in italics (four Sta. 5, 11, 12, and 33).

Western Brittany, Central Bay of Biscay, Arcachon Lagoon, Gulf of Lion, and 47–70% for Northern Bay of Biscay and English Channel (but all western English Channel stations were correlated, Table 2). When comparing station pairs between regions, there was an increase in correlation from north to south: the English Channel stations were poorly correlated with stations from the other regions (29–42%) while the Gulf of Lion, the Central Bay of Biscay and the Arcachon Lagoon showed more correlations (60–87%) between station pairs.

Correlations between bivalve-$\delta^{13}C$ and global proxies

Bivalve-$\delta^{13}C$ was positively correlated with $\delta^{13}C$-CO_{2aq} for 78% of the stations (Table 3). Both $\delta^{13}C$ decreased concomitantly over time. There was a negative correlation between bivalve-$\delta^{13}C$ and CO_{2atm} and NHT for 78% and 75% of the stations respectively. The higher the atmospheric CO_2 concentrations and the warmer the air temperatures (positive anomalies) in the Northern hemisphere, the more negative were bivalve-$\delta^{13}C$ values. The EAP (pressure) and AMO (temperature) indices were negatively correlated with

Table 2. Correlation matrix between station pairs for bivalves $\delta^{13}C$ (bivalve-$\delta^{13}C$, lower half triangle, dark gray) and bivalves $\delta^{13}C$ corrected for Suess effect (bivalve-$\delta^{13}C_{corr}$, upper half triangle, light gray).

		English Channel (EC)									Western Brittany (WB)				Northern Bay of Biscay (NB)				
	$\delta^{13}C_{corr}$ $\delta^{13}C$	EC-1-AMBL	EC-2-PSQT	EC-3-VARE	EC-4-ANTI	EC-5-CLHV	EC-6-VILL	EC-7-OUIS	EC-8-PBES	EC-9-BDVG	WB-10-PLAN	WB-11-PASS	WB-12-PERS	WB-13-AULN	NB-14-GUIL	NB-15-PEBE	NB-16-CHEM	NB-18-BOUR	NB-19-NOIR
English Channel (EC)	EC-1-AMBL																		
	EC-2-PSQT	0.42															0.47		
	EC-3-VARE																		
	EC-4-ANTI					0.85	0.75	0.50		0.48		0.69							
	EC-5-CLHV				0.83		0.76												
	EC-6-VILL				0.73	0.74		0.49		0.58									
	EC-7-OUIS	0.55			0.65		0.61		0.71	0.79	0.55	0.56	0.73						
	EC-8-PBES	0.54		0.38	0.52		0.57	0.81		0.76									
	EC-9-BDVG	0.54			0.61		0.65	0.85	0.84										
Western Brittany (WB)	WB-10-PLAN				0.44			0.65	0.55	0.62		0.74	0.77						
	WB-11-PASS				0.78		0.59	0.62		0.6	0.79				0.83				0.46
	WB-12-PERS				0.61		0.57	0.74		0.52	0.84	0.71			0.62				0.48
	WB-13-AULN							0.48	0.46	0.48	0.61		0.51					0.39	
Northern Bay of Biscay (NB)	NB-14-GUIL				0.4			0.60		0.44	0.52	0.86	0.75			0.52			0.36
	NB-15-PEBE				0.39	0.45	0.39				0.39	0.69	0.54		0.51			0.41	0.43
	NB-16-CHEM					0.5										0.4			
	NB-18-BOUR						0.43		0.46	0.37	0.52			0.59	0.35	0.56			0.36
	NB-19-NOIR							0.53	0.45	0.43	0.59	0.55	0.58	0.36	0.53	0.57		0.56	
Central Bay of Biscay (CB)	CB-20-RIVE				0.42			0.77	0.68	0.69	0.84	0.78	0.63	0.56	0.54	0.37		0.60	0.73
	CB-21-PALL						0.43	0.50	0.57	0.58	0.57			0.39		0.44		0.63	0.54
	CB-22-BOYV							0.40	0.54	0.55	0.75			0.55	0.39	0.39		0.59	0.65
	CB-23-PONT				0.44		0.4	0.53	0.46	0.60	0.51	0.49		0.44	0.49	0.44		0.61	0.46
	CB-24-FOSS				0.44					0.38									
Arcachon lagoon (AL)	AL-25-FERR														0.37			0.39	0.37
	AL-26-JACQ				0.62	0.45	0.53	0.49	0.44	0.44	0.52	0.51			0.42			0.42	
	AL-27-COMP	0.51			0.41			0.75	0.68	0.71	0.74	0.55		0.42	0.41			0.48	0.54
Gulf of lion (GL)	GL-28-BANY									0.54	0.67			0.44					0.52
	GL-29-HRLT										0.56								
	GL-30-STMM	0.41		0.45				0.55	0.49	0.49	0.76			0.51	0.46	0.45		0.64	0.50
	GL-31-CART	0.4						0.40		0.46	0.66	0.53			0.51			0.37	0.44
	GL-32-COUR	0.45			0.4			0.76	0.62	0.73	0.84	0.73	0.62	0.48	0.53			0.51	0.55
	GL-33-POME	0.47						0.51		0.47					0.48		–0.52		

	Central Bay of Biscay (CB)					Arcachon lagoon (AL)			Gulf of lion (GL)					
	CB-20-RIVE	CB-21-PALL	CB-22-BOYV	CB-23-PONT	CB-24-FOSS	AL-25-FERR	AL-26-JACQ	AL-27-COMP	GL-28-BANY	GL-29-HRLT	GL-30-STMM	GL-31-CART	GL-32-COUR	GL-33-POME
English Channel (EC)	–0.46		–0.50											
							0.52							
			–0.42											
	0.69							0.67			0.40		0.61	
	0.55		0.36					0.60						
	0.48							0.61					0.51	
Western Brittany (WB)	0.71		0.59					0.6			0.57	0.5	0.7	
	0.7												0.61	
Northern Bay of Biscay (NB)			–0.42											–0.66
				0.44							0.36			
	0.55		0.42											
Central Bay of Biscay (CB)		0.44	0.75	0.46				0.58				0.47	0.62	
	0.65		0.52	0.45				0.43						
	0.87	0.73		0.42				0.51	0.51			0.35	0.49	0.43
	0.65	0.59	0.58		0.74			0.51						
	0.38	0.41		0.78			0.5							
Arcachon lagoon (AL)		0.37	0.47	0.49										
	0.43	0.41	0.40	0.57	0.56	0.55		0.44						
	0.73	0.7	0.75	0.65	0.46	0.63	0.65						0.76	
Gulf of lion (GL)	0.59		0.68					0.58		0.62		0.52	0.58	
			0.47					0.42	0.76					
	0.62	0.41	0.57	0.41		0.43	0.42	0.59	0.42	0.44		0.5	0.64	
	0.66		0.60	0.41		0.38		0.64	0.71	0.43	0.61		0.71	
	0.78	0.6	0.72	0.59		0.5	0.53	0.86	0.75	0.59	0.76	0.82		
	0.64	0.49	0.56	0.46				0.63				0.61	0.69	

Only significant correlations are shown (two-sided Spearman tests rho values [rank correlation coefficient]; *p*-value <0.05).

bivalve-$\delta^{13}C$ for 56% and 44% of the stations respectively. Positive phases of both EAP and AMO, which increase sea surface temperature and are linked to milder and wetter precipitation in winter months over most of Northern Europe, were linked to more negative bivalve-$\delta^{13}C$ values. There was no significant correlation between bivalve-$\delta^{13}C$ and AO and NAO. Regionally, the English Channel and Northern Bay of Biscay showed less correlations (47% and 40%, respectively) with global proxies (out of AO, NAO, and $\delta^{13}C$-CO_{2atm}) than the Gulf of Lion and Arcachon Lagoon (87%) (Table 3).

Remaining pluri-decadal trends in Suess-corrected bivalve-$\delta^{13}C$

After removing the Suess effect from bivalve-$\delta^{13}C$ trends, we tested the significance of the remaining trends. Over the common period of 30 ± 2 yr (1990–2021), bivalve-$\delta^{13}C_{corr}$ significantly decreased for 50% of the stations, while 46% exhibited no significant change, and one station experienced a significant increase (EC-2-PSQT) (Table 1). The average decrease was −0.45 ± 0.27‰ decade^{-1} ranging from −0.84 to −0.19‰ decade^{-1} (from −2.52 to −0.58‰ over 30 years). There were only 28–50% significant correlations in bivalve-$\delta^{13}C_{corr}$ between station pairs within each region except for Central Bay of Biscay (70%; Table 2). There was almost no correlation remaining between station pairs of different regions (0–33%; Table 2).

Remaining correlations between Suess-corrected bivalve-$\delta^{13}C$ and global proxies

Overall, the number of correlations with global proxies decreased after removing the Suess effect. Bivalve-$\delta^{13}C_{corr}$ was still correlated with $\delta^{13}C$-CO_{2aq} at 53% of the stations, mostly positively (negatively correlated at two stations; Table 3). There were 47–53% correlations left between bivalve-$\delta^{13}C_{corr}$ and NHT and CO_{2atm}, mostly negative, and only 25–34% correlations remained for the other hydro-climatic indices. Still, there was no significant correlation between bivalve-$\delta^{13}C_{corr}$, and AO and NAO. Regionally, more correlations were remaining with global proxies (55–60%, out of AO NAO and $\delta^{13}C$-CO_{2atm}) for Western Brittany and Gulf of Lion than for the other regions (28–44%).

Discussion

We found an overall global temporal decrease in bivalves $\delta^{13}C$ tissues in all sea regions, independently of bivalve species and despite differences in trophic status, tidal regime, continental influence, etc., of the studied ecosystems (Lheureux et al. 2023). This decrease was of same order of magnitude in all regions and with numerous correlations between stations of different sea regions. These results are consistent with the literature regarding marine organisms from different trophic levels (e.g., Druffel and Benavides 1986; Aharon 1991; Bauch et al. 2000; Schloesser et al. 2009) including bivalve species from other sea areas (Liénart et al. 2022, −0.45‰ decade^{-1}). The decrease in bivalve-$\delta^{13}C$ correlates in all regions with the global decrease in $\delta^{13}C$ of dissolved CO_2 linked to the Suess effect (Keeling 1979). Among global processes directly altering bivalve-$\delta^{13}C$, the Suess effect can be measured, and therefore removed from pluri-decadal trends. After its correction, 46% of previous bivalve-$\delta^{13}C$ slopes were not significant anymore and there were almost no correlations left between regions, showing that part of global direct anthropogenic effect on bivalve-$\delta^{13}C$ was removed. Yet, significant decrease in bivalve-$\delta^{13}C_{corr}$ was still observed for 50% of the stations, and up to 60% of correlations with other global proxies remained in some regions (Gulf of Lion), indicating that other global processes affecting bivalve-$\delta^{13}C$ values are still ongoing.

In addition to the Suess effect, increasing temperatures and CO_2 concentrations affect bivalve-$\delta^{13}C$ via trophic pathway (Corman et al. 2018). Indeed, even after the Suess-effect correction, a large proportion of stations still exhibited negative correlation between bivalve-$\delta^{13}C_{corr}$, atmospheric CO_2 concentration and NHT (both proxies for anthropogenic activities), and with AMO and EAP (proxies for natural climate, which trends indicate increased surface temperatures in Northern Atlantic; Comas-Bru and McDermott 2014; Zampieri et al. 2017). Changes in phytoplankton physiology and community assemblages can also both explain the decrease in bivalve-$\delta^{13}C$ over time. Carbon isotope fractionation (i.e., enrichment of one isotope relative to another during [bio]chemical or physical processes) between phytoplankton and dissolved CO_2 is modulated by the balance between carbon demand (i.e., productivity/growth rate) and CO_2 availability (Fry 1996): as the increase in water temperature increases carbon demand (productivity) and decreases dissolved CO_2 concentration (CO_2 availability), phytoplankton isotopic fractionation decreases, leading to an overall increase in phytoplankton-$\delta^{13}C$; in contrast, as atmospheric and seawater CO_2 concentration increase due to fossil fuel burning, phytoplankton isotopic fractionation increases, leading to a decrease in phytoplankton-$\delta^{13}C$. Additionally, temperature increase may change phytoplankton community toward smaller cell-sized species (e.g., David et al. 2012; Hernández-Fariñas et al. 2014), which display lower $\delta^{13}C$ values (e.g., Tuerena et al. 2019). All these processes are likely to occur concomitantly and reflect into bivalve tissues as any changes in phytoplankton-$\delta^{13}C$ directly alter bivalve-$\delta^{13}C$ by trophic propagation (Lefebvre et al. 2009).

Global change also affects bivalve-$\delta^{13}C$ through bivalve physiology. Bivalve isotope fractionation directly relates to metabolic rates, (e.g., assimilation and growth, Lefebvre and Dubois 2016) which are temperature-dependent (Hiebenthal et al. 2013; Matoo et al. 2021). In their study, Marín Leal et al. (2008) showed that lower $\delta^{13}C$ during winter were associated with lower metabolic rate. Increasing water temperature over

Table 3. Correlations between global anthropogenic and climate proxies, and both bivalve $\delta^{13}C$ (bivalve-$\delta^{13}C$, left panel, dark gray) and bivalves $\delta^{13}C$ corrected for the Suess effect (bivalve-$\delta^{13}C_{corr}$, right panel, light gray) for each station of the six sea regions.

		Bivalve-$\delta^{13}C$								Bivalve-$\delta^{13}C_{corr}$							
		AO	NAO	AMO	EAP	NHT	CO_{2atm}	$\delta^{13}C_{atm}$	$\delta^{13}C_{aq}$	AO	NAO	AMO	EAP	NHT	CO_{2atm}	$\delta^{13}C_{atm}$	$\delta^{13}C_{aq}$
English Channel (EC)	EC-1-AMBL						−0.39	0.39	0.39								
	EC-2-PSQT													0.39	0.46	−0.45	−0.45
	EC-3-VARE																
	EC-4-ANTI				−0.47	−0.41	−0.43	0.43	0.43								
	EC-5-CLHV																
	EC-6-VILL				−0.55								−0.4				
	EC-7-OUIS				−0.47	−0.68	−0.79	0.79	0.79				−0.46	−0.62	−0.74	0.74	0.74
	EC-8-PBES			−0.46	−0.5	−0.68	−0.72	0.72	0.72				−0.4	−0.54	−0.56	0.57	0.57
	EC-9-BDVG			−0.43	−0.57	−0.65	−0.67	0.67	0.67				−0.48	−0.39	−0.37	0.37	0.37
Western Bretagne (WB)	WB-10-PLAN			−0.65	−0.58	−0.82	−0.88	0.88	0.88			−0.61	−0.56	−0.75	−0.81	0.8	0.8
	WB-11-PASS				−0.51	−0.67	−0.8	0.8	0.8				−0.59	−0.66	−0.75	0.75	0.75
	WB-12-PERS					−0.54	−0.68	0.68	0.68						−0.53	0.53	0.53
	WB-13-AULN			−0.47		−0.56	−0.56	0.57	0.57								
Northern Bay of Biscay (NB)	NB-14-GUIL					−0.37	−0.53	0.52	0.52								
	NB-15-PEBE																
	NB-16-CHEM											0.49		0.53	0.56	−0.56	−0.56
	NB-18-BOUR			−0.37		−0.53	−0.58	0.58	0.58								
	NB-19-NOIR			−0.42	−0.38	−0.65	−0.69	0.69	0.69					−0.43	−0.44	0.44	0.44
Central Bay of Biscay (MB)	CB-20-RIVE			−0.65	−0.49	−0.81	−0.88	0.88	0.88			−0.57	−0.46	−0.73	−0.79	0.78	0.78
	CB-21-PALL			−0.5	−0.59	−0.64	−0.58	0.58	0.58				−0.44				
	CB-22-BOYV			−0.73	−0.45	−0.82	−0.88	0.88	0.88			−0.66	−0.38	−0.73	−0.77	0.77	0.77
	CB-23-PONT				−0.38	−0.45	−0.56	0.55	0.55								
	CB-24-FOSS																
Arcachon lagoon (AL)	AL-25-FERR				−0.38	−0.41	−0.51	0.49	0.49								
	AL-26-JACQ				−0.43	−0.38	−0.49	0.47	0.47								
	AL-27-COMP			−0.53	−0.54	−0.72	−0.79	0.78	0.78			−0.35	−0.47	−0.55	−0.62	0.62	0.62
Gulf of lion (GL)	GL-28-BANY			−0.65	−0.38	−0.69	−0.75	0.75	0.75			−0.54		−0.52	−0.59	0.58	0.58
	GL-29-HRLT			−0.45		−0.52	−0.51	0.52	0.52								
	GL-30-STMM			−0.46	−0.41	−0.64	−0.73	0.73	0.73					−0.42	−0.52	0.52	0.52
	GL-31-CART			−0.61		−0.62	−0.74	0.73	0.73			−0.49		−0.46	−0.58	0.56	0.56
	GL-32-COUR			−0.69	−0.49	−0.81	−0.89	0.89	0.89			−0.59	−0.4	−0.68	−0.76	0.75	0.75
	GL-33-POME					−0.53	−0.7	0.7	0.7						−0.54	0.54	0.54

Only significant correlations are shown (two-sided Spearman tests rho values [rank correlation coefficient]; *p*-values < 0.05).

multidecadal scales should result in increased metabolic activity, hence in bivalves-$\delta^{13}C$ as a pure metabolic effect. In addition, lipid content in bivalves (reflected by higher C:N ratio when it increases) should decrease with warmer temperatures in temperate regions (Tan et al. 2023) translating to increased bivalves-$\delta^{13}C$ values and decreased C:N (Post et al. 2007). However, this is not the observed trend (decreasing bivalve-$\delta^{13}C$, no overall decreasing trend in C:N ratio; data not shown), which suggests that bivalve physiology is likely not a dominant process for the multidecadal bivalve-$\delta^{13}C$ trends of this study. These trends are rather explained by direct (through diet) or indirect (through the effect of abiotic factors on phytoplankton physiology) changes in bivalve-$\delta^{13}C$ through food availability and quality (Liénart et al. 2020, 2023).

As these effects are linked to global drivers, they should similarly affect all regions and stations. However, 'only' 50% of the stations still exhibit significant decrease in Suess-corrected bivalves-$\delta^{13}C$ (most of the stations of Western Brittany, Central Bay of Biscay and Gulf of Lion) and only 43% of the stations still exhibit a correlation between bivalves-$\delta^{13}C_{corr}$ and global proxies (out of AO NAO and $\delta^{13}C$-CO_{2atm}; most of the stations of Western Brittany and Gulf of Lion). This indicates that beyond global drivers, bivalves-$\delta^{13}C$ also responds to regional/local drivers that have cumulative, synergetic (for the stations exhibiting more negative slopes) or antagonistic (for the stations exhibiting less negative slope, nonsignificant or even positive slope) effect with global drivers. It is beyond the scope of this article to discuss these regional/local drivers but the present results clearly enlighten their effect on bivalves-$\delta^{13}C$.

To summarize, the global increase in atmospheric CO_2 has many impacts (e.g., global warming), including on marine ecosystems (e.g., increased seawater temperature, increased primary production). Such changes go beyond physical–chemical processes or changes in the production base and have an impact on species at the base of the food webs, with potential knock-on effects expected on upper trophic levels, including isotopic signal. Our study demonstrates that the changes in the chemical composition of the atmosphere (increase in CO_2 and associated decrease in $\delta^{13}C$-CO_{2atm}) are recorded in bivalves soft-tissues. This global effect is likely related to 'passive' processes (Suess effect; changes in $\delta^{13}C$-CO_{2atm} directly modify bivalve-$\delta^{13}C$ through physical and chemical processes, i.e., without change in biological processes), but is also associated to 'active' processes (i.e., biological, due to change in phytoplankton or bivalve fractionation and physiology). Indeed, even after removing the Suess effect, a link between bivalve-$\delta^{13}C$ and global indices remains for half of the stations. Beyond global effect, regional and/or local effects likely occur in cumulative, synergistic or antagonistic ways. Correcting $\delta^{13}C$ time series for the Suess effect is a first and necessary step required when comparing biological samples collected one or more decades apart (as previously advised by Misarti et al. 2009; Dombrosky 2020; Clark et al. 2021). Further studies are required to comprehensively investigate regional/local processes related to changes in bivalve-$\delta^{13}C$ once corrected for the Suess effect, which will contribute to a deeper understanding of ecosystem responses to global change.

Funding Information

This work is part of the research project EVOLECO-BEST funded by the Office Français de la Biodiversité (OFB).

References

Affek, H. P., and D. Yakir. 2014. The stable isotopic composition of atmospheric CO_2, p. 179–212. *In* H. D. Holland and K. K. Turekian [eds.], *Treatise on geochemistry*, v. **5**, Second ed. Elsevier. doi:10.1016/B978-0-08-095975-7.00407-1

Aharon, P. 1991. Recorders of reef environment histories: Stable isotopes in corals, giant clams, and calcareous algae. Coral Reefs **10**: 71–90. doi:10.1007/BF00571826

Barbier, E. B., S. D. Hacker, C. Kennedy, E. W. Koch, A. C. Stier, and B. R. Silliman. 2011. The value of estuarine and coastal ecosystem services. Ecol. Monogr. **81**: 169–193. doi:10.1890/10-1510.1

Barnston, A. G., and R. E. Livezey. 1987. Classification, seasonality and persistence of low-frequency atmospheric circulation patterns. Mon. Weather Rev. **115**: 1083–1126. doi:10.1175/1520-0493(1987)115<1083:CSAPOL>2.0.CO;2

Bartley, T. J., and others. 2019. Food web rewiring in a changing world. Nat. Ecol. Evol. **3**: 345–354. doi:10.1038/s41559-018-0772-3

Bauch, D., J. Carstens, G. Wefer, and J. Thiede. 2000. The imprint of anthropogenic CO_2 in the Arctic Ocean: Evidence from planktic $\delta^{13}C$ data from water column and sediment surfaces. Deep Res. Part II Top. Stud. Oceanogr. **47**: 1791–1808. doi:10.1016/S0967-0645(00)00007-2

Bauer, J. E., W.-J. Cai, P. A. Raymond, T. S. Bianchi, C. S. Hopkinson, and P. A. G. Regnier. 2013. The changing carbon cycle of the coastal ocean. Nature **504**: 61–70. doi:10.1038/nature12857

Benedetti, F., M. Vogt, U. H. Elizondo, D. Righetti, N. E. Zimmermann, and N. Gruber. 2021. Major restructuring of marine plankton assemblages under global warming. Nat. Commun. **12**: 1–15. doi:10.1038/s41467-021-25385-x

Briant, N., and others. 2018. Carbon and nitrogen elemental and isotopic ratios of filter-feeding bivalves along the French coasts: An assessment of specific, geographic, seasonal and multi-decadal variations. Sci. Total Environ. **613–614**: 196–207. doi:10.1016/j.scitotenv.2017.08.281

Briant, N., P. Le Monier, S. Bruzac, T. Sireau, D. F. Araújo, and A. Grouhel. 2021. Rare earth element in bivalves' soft tissues of French metropolitan coasts: Spatial and temporal distribution. Arch. Environ. Contam. Toxicol. **81**: 600–611. doi:10.1007/s00244-021-00821-7

Bristow, L. A., T. D. Jickells, K. Weston, A. Marca-Bell, R. Parker, and J. E. Andrews. 2013. Tracing estuarine organic matter sources into the southern North Sea using C and N isotopic signatures. Biogeochemistry **113**: 9–22. doi:10.1007/s10533-012-9758-4

Cabral, H., V. Fonseca, T. Sousa, and M. C. Leal. 2019. Synergistic effects of climate change and marine pollution: An overlooked interaction in coastal and estuarine areas. Int. J. Environ. Res. Public Health **16**: 1–17. doi:10.3390/ijerph16152737

Cael, B. B., K. Bisson, E. Boss, S. Dutkiewicz, and S. Henson. 2023. Global climate change trends detected in indicators of ocean ecology. Nature **619**: 551–554. doi:10.1038/s41586-023-06321-z

Chahouri, A., B. Yacoubi, A. Moukrim, and A. Banaoui. 2023. Bivalve molluscs as bioindicators of multiple stressors in the marine environment: Recent advances. Cont. Shelf Res. **264**: 105056. doi:10.1016/j.csr.2023.105056

Clark, C. T., M. R. Cape, M. D. Shapley, F. J. Mueter, B. P. Finney, and N. Misarti. 2021. SuessR: Regional corrections for the effects of anthropogenic CO_2 on $\delta^{13}C$ data from marine organisms. Methods Ecol. Evol. **12**: 1508–1520. doi:10.1111/2041-210X.13622

Comas-Bru, L., and F. Mcdermott. 2014. Impacts of the EA and SCA patterns on the European twentieth century NAO-winter climate relationship. Q. J. Roy. Meteorol. Soc. **140**: 354–363. doi:10.1002/qj.2158

Corman, A. M., and others. 2018. Decreasing $\delta^{13}C$ and $\delta^{15}N$ values in four coastal species at different trophic levels indicate a fundamental food-web shift in the southern north and Baltic seas between 1988 and 2016. Environ. Monit. Assess. **190**: 1–12. doi:10.1007/s10661-018-6827-8

David, V., M. Ryckaert, M. Karpytchev, C. Bacher, V. Arnaudeau, N. Vidal, D. Maurer, and N. Niquil. 2012. Spatial and long-term changes in the functional and structural phytoplankton communities along the French Atlantic coast. Estuar. Coast. Shelf Sci. **108**: 37–51. doi:10.1016/j.ecss.2012.02.017

Dombrosky, J. 2020. A ~1000-year ^{13}C Suess correction model for the study of past ecosystems. Holocene **30**: 474–478. doi:10.1177/0959683619887416

Druffel, E. R. M., and L. M. Benavides. 1986. Input of excess CO_2 to the surface ocean based on $^{13}C/^{12}C$ ratios in a banded Jamaican sclerosponge. Nature **321**: 58–61. doi:10.1038/321058a0

Enfield, D. B., A. M. Mestas-Nuñez, and P. J. Trimble. 2001. The Atlantic multidecadal oscillation and its relation to rainfall and river flows in the continental U.S. Geophys. Res. Lett. **28**: 2077–2080. doi:10.1029/2000GL012745

Fry, B. 1996. $^{13}C/^{12}C$ fractionation by marine diatoms. Mar. Ecol. Prog. Ser. **134**: 283–294. doi:10.3354/meps134283

Gittings, J. A., D. E. Raitsos, G. Krokos, and I. Hoteit. 2018. Impacts of warming on phytoplankton abundance and phenology in a typical tropical marine ecosystem. Sci. Rep. **8**: 2240. doi:10.1038/s41598-018-20560-5

Graven, H., and others. 2017. Compiled records of carbon isotopes in atmospheric CO_2 for historical simulations in CMIP6. Geosci. Model Dev. **10**: 4405–4417. doi:10.5194/gmd-10-4405-2017

Gruber, N., and others. 1999. Spatiotemporal patterns of carbon-13 in the global surface ocean and the oceanic Suess effect. Global Biogeochem. Cycles **13**: 307–335. doi:10.1029/1999GB900019

Halpern, B. S., and others. 2008. A global map of human impact on marine ecosystems. Science **319**: 948–952. doi:10.1126/science.1149345

Harley, C. D. G., and others. 2006. The impacts of climate change in coastal marine systems. Ecol. Lett. **9**: 228–241. doi:10.1111/j.1461-0248.2005.00871.x

Hernández-Fariñas, T., and others. 2014. Temporal changes in the phytoplankton community along the French coast of the eastern English Channel and the southern bight of the North Sea. ICES J. Mar. Sci. **71**: 821–833. doi:10.4135/9781412953924.n678

Hiebenthal, C., E. E. R. Philipp, A. Eisenhauer, and M. Wahl. 2013. Effects of seawater pCO_2 and temperature on shell growth, shell stability, condition and cellular stress of Western Baltic Sea *Mytilus edulis* (L.) and *Arctica islandica* (L.). Mar. Biol. **160**: 2073–2087. doi:10.1007/s00227-012-2080-9

Higgins, R. W., A. Leetmaa, Y. Xue, and A. Barnston. 2000. Dominant factors influencing the seasonal predictability of U.S. precipitation and surface air temperature. J. Climate **13**: 3994–4017. doi:10.1175/1520-0442(2000)013<3994:DFITSP>2.0.CO;2

Hurrell, J. W. 1995. Decadal trends in the North Atlantic oscillation: Regional temperatures and precipitation. Science **269**: 676–679. doi:10.1126/science.269.5224.676

Hurrell, J. W., and C. Deser. 2009. North Atlantic climate variability: The role of the North Atlantic oscillation. J. Mar. Syst. **78**: 28–41. doi:10.1016/j.jmarsys.2008.11.026

Karlson, A. M. L., and S. Faxneld. 2021. Polycyclic aromatic hydrocarbons and stable isotopes of carbon and nitrogen in Baltic Sea blue mussels: Time series data 1981–2016. Data Br. **35**: 4–8. doi:10.1016/j.dib.2021.106777

Keeling, C. D. 1979. The Suess effect: ^{13}Carbon-^{14}Carbon interrelations. Environ. Int. **2**: 229–300. doi:10.1016/0160-4120(79)90005-9

Lan, X., P. Tans, and K. W. Thoning. 2023. Trends in globally-averaged CO_2 determined from NOAA global monitoring laboratory measurements. Version 2023-04. doi:10.15138/9N0H-ZH07

Lefebvre, S., J. C. Marín Leal, S. Dubois, F. Orvain, J.-L. Blin, M.-P. Bataillé, A. Ourry, and R. Galois. 2009. Seasonal dynamics of trophic relationships among co-occurring suspension feeders in two shellfish culture dominated ecosystems. Estuar. Coast. Shelf Sci. **82**: 415–425. doi:10.1016/j.ecss.2009.02.002

Lefebvre, S., and S. F. Dubois. 2016. The stony road to understand isotopic enrichment and turnover rates: Insight into

the metabolic part. Vie Milieu Life Environ. **66**: 305–314 https://archimer.ifremer.fr/doc/00387/49856/

Lheureux, A., and others. 2023. Trajectories of nutrients concentrations and ratios in the French coastal ecosystems: 20 years of changes in relation with large-scale and local drivers. Sci. Tot. Environ. **857**: 159619. doi:10.1016/j.scitotenv.2022.159619

Liénart, C., and others. 2017. Dynamics of particulate organic matter composition in coastal systems: A spatio-temporal study at multi-system scale. Prog. Oceanogr. **156**: 221–239. doi:10.1016/j.pocean.2017.03.001

Liénart, C., and others. 2020. Long-term changes in trophic ecology of blue mussels in a rapidly changing ecosystem. Limnol. Oceanogr. **66**: 694–710. doi:10.1002/lno.11633

Liénart, C., A. Garbaras, S. Qvarfordt, H. Lim, M. Chynel, C. Robinson, T. Meziane, and A. M. L. Karlson. 2022. Spatio-temporal variation in stable isotope and elemental composition of key-species reflect environmental changes in the Baltic Sea. Biogeochemistry **157**: 149–170. doi:10.1007/s10533-021-00865-w

Liénart, C., M. Tedengren, A. Garbaras, H. Lim, M. Chynel, C. Robinson, T. Meziane, and A. M. L. Karlson. 2023. Diet quality determines blue mussel physiological status: A long-term experimental multi-marker approach. J. Exp. Mar. Biol. Ecol. **563**: 151894. doi:10.1016/j.jembe.2023.151894

Magni, P., S. Rajagopal, S. Como, J. M. Jansen, G. van der Velde, and H. Hummel. 2013. $\delta^{13}C$ and $\delta^{15}N$ variations in organic matter pools, *Mytilus* spp. and *Macoma balthica* along the European Atlantic coast. Mar. Biol. **160**: 541–552. doi:10.1007/s00227-012-2110-7

Marín Leal, J. C., and others. 2008. Stable isotopes (δ13C, δ15N) and modelling as tools to estimate the trophic ecology of cultivated oysters in two contrasting environments. Mar. Biol. **153**: 673–688. doi:10.1007/s00227-007-0841-7

Matoo, O. B., G. Lannig, C. Bock, and I. M. Sokolova. 2021. Temperature but not ocean acidification affects energy metabolism and enzyme activities in the blue mussel, *Mytilus edulis*. Ecol. Evol. **11**: 336–3379. doi:10.1002/ece3.7289

Milliman, J. D., K. L. Farnsworth, P. D. Jones, K. H. Xu, and L. C. Smith. 2008. Climatic and anthropogenic factors affecting river discharge to the global ocean, 1951-2000. Glob. Planet. Change **62**: 187–194. doi:10.1016/j.gloplacha.2008.03.001

Misarti, N., B. Finney, H. Maschner, and M. J. Wooller. 2009. Changes in northeast Pacific marine ecosystems over the last 4500 years: Evidence from stable isotope analysis of bone collagen from archeological middens. Holocene **19**: 1139–1151. doi:10.1177/0959683609357824

Mook, W. G. 2000. *Environmental isotopes in the hydrological cycle: Principles and applications*. UNESCO.

Patakamuri, S., and N. O'Brien. 2021. Modifiedmk: Modified versions of Mann Kendall and Spearman's rho trend tests. R package version 1.6. https://CRAN.R-project.org/package=modifiedmk

Post, D. M., C. A. Layman, D. A. Arrington, G. Takimoto, J. Quattrochi, and C. G. Montaña. 2007. Getting to the fat of the matter: Models, methods and assumptions for dealing with lipids in stable isotope analyses. Oecologia **152**: 179–189. doi:10.1007/s00442-006-0630-x

Pörtner, H. O., M. Langenbuch, and B. Michaelidis. 2005. Synergistic effects of temperature extremes, hypoxia, and increases in CO_2 on marine animals: From earth history to global change. J. Geophys. Res. Ocean. **110**: 1–15. doi:10.1029/2004JC002561

Quay, P., R. Sonnerup, J. Stutsman, J. Maurer, A. Körtzinger, X. A. Padin, and C. Robinson. 2007. Anthropogenic CO_2 accumulation rates in the North Atlantic Ocean from changes in the $^{13}C/^{12}C$ of dissolved inorganic carbon. Global Biogeochem. Cycles **21**: 1–15. doi:10.1029/2006GB002761

R Core Team. 2022. *R: A language and environment for statistical computing*. R Foundation for Statistical Computing, https://www.R-project.org/

Schloesser, R. W., J. R. Rooker, P. Louchuoarn, J. D. Neilson, and D. H. Secor. 2009. Interdecadal variation in seawater $\delta^{13}C$ and $\delta^{18}O$ recorded in fish otoliths. Limnol. Oceanogr. **54**: 1665–1668. doi:10.4319/lo.2009.54.5.1665

Tan, K., J. Ransangan, K. Tan, and K. L. Cheong. 2023. The impact of climate change on Omega-3 long-chain polyunsaturated fatty acids in bivalves. Crit. Rev. Food Sci. Nutr.: 1–11. doi:10.1080/10408398.2023.2242943

Tuerena, R. E., R. S. Ganeshram, M. P. Humphreys, T. J. Browning, H. Bouman, and A. P. Piotrowski. 2019. Isotopic fractionation of carbon during uptake by phytoplankton across the South Atlantic subtropical convergence. Biogeosciences **16**: 3621–3635. doi:10.5194/bg-16-3621-2019

Vander Zanden, M. J., and J. B. Rasmussen. 1999. Primary consumer $\delta^{13}C$ and $\delta^{15}N$ and the trophic position of aquatic consumers. Ecology **80**: 1395–1404. doi:10.1890/0012-9658(1999)080[1395:PCCANA]2.0.CO;2

van Vliet, M. T., W. H. Franssen, J. R. Yearsley, F. Ludwig, I. Haddeland, D. P. Lettenmaier, and P. Kabat. 2013. Global river discharge and water temperature under climate change. Glob. Environ. Chang. **23**: 450–464. doi:10.1016/j.gloenvcha.2012.11.002

Vogel, J. C., P. M. Grootes, and W. G. Mook. 1970. Isotope fractionation between gaseous and dissolved carbon dioxide. Z. Phys. **230**: 225–238. doi:10.1007/BF01394688

Zampieri, M., A. Toreti, A. Schindler, and S. Gualdi. 2017. Atlantic multi-decadal oscillation influence on weather regimes over Europe and the Mediterranean in spring and summer. Glob. Planet. Change **151**: 92–100. doi:10.1016/j.gloplacha.2016.08.014

Zeebe, R. E., and D. Wolf-Gladrow. 2001. *CO_2 in seawater: Equilibrium, kinetics, isotopes*, v. **65**. Elsevier Oceanography Series, p. 1–346.

Acknowledgments

This article is based on a collaborative work with the team of the ROCCH monitoring network (Ifremer). We thank the members of the ROCCH and of the different institutions, from the field workers and analysts to the coordinators, who made the use of the data possible. We would like to thank the different laboratories teams of the National Oceanic and Atmospheric Administration for producing atmospheric and teleconnection indices data. We would like to thank the anonymous reviewers for their valuable work that helped in improving this manuscript. This work is part of the research project EVOLECO-BEST funded by the Office Français de la Biodiversité (OFB).

Submitted 17 October 2023
Revised 10 April 2024
Accepted 14 April 2024